Matter

CellPress

Article

The strongest and toughest predicted materials: Linear atomic chains without a Peierls instability

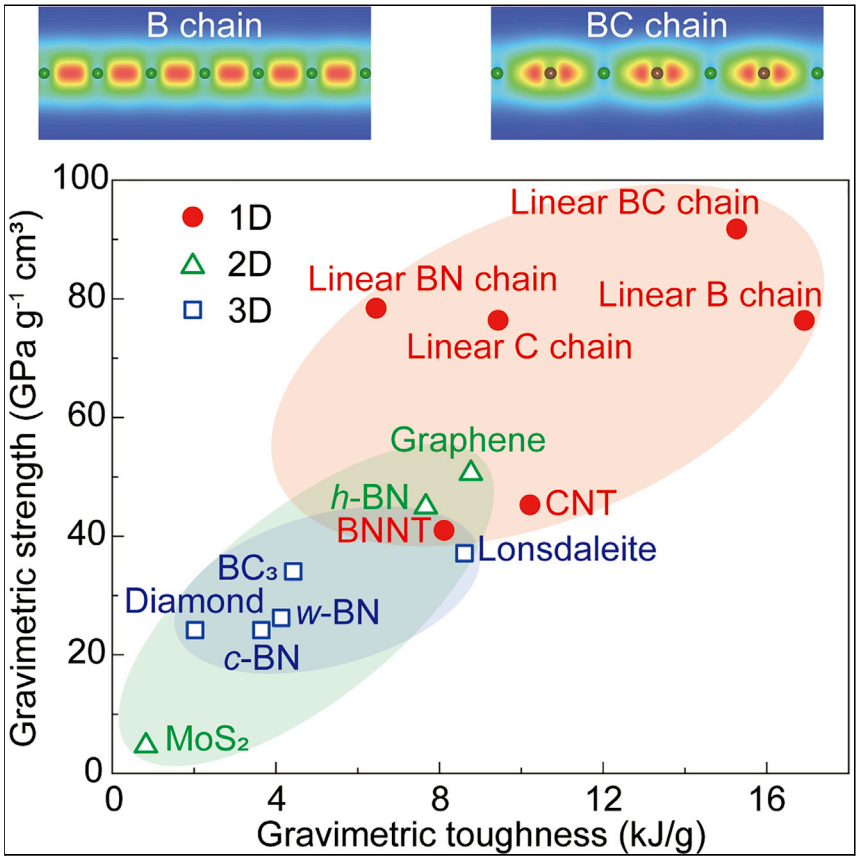

In this study, we predicted the properties of B, C, N, BC, BN, and CN linear atomic chains by first-principles calculations. We computationally found that B chains have the highest recorded gravimetric toughness, whereas BC chains have the highest recorded gravimetric strength and high toughness. Electronic structure analyses show that the higher strength and toughness of the BC and B chains, compared with carbyne, originate from their strong chemical bonding and the absence of a Peierls instability during stretching.

Discovery
A new material or phenomena

Enlai Gao, Yongzhe Guo, Zhengzhi Wang, Steven O. Nielsen, Ray H. Baughman

enlaigao@whu.edu.cn (E.G.)
zhengzhi.wang@whu.edu.cn (Z.W.)
ray.baughman@utdallas.edu (R.H.B.)

Highlights

Linear B, C, BC, and BN chains are stable when under tension at room temperature

Linear BC and B chains have the highest recorded gravimetric strength and toughness

The mechanism is the strong bonding and the absence of a Peierls instability

Gao et al., Matter 5, 1192–1203
April 6, 2022
https://doi.org/10.1016/j.matt.2022.01.021

CellPress

Matter

Article

The strongest and toughest predicted materials: Linear atomic chains without a Peierls instability

Enlai Gao,[1,2,5,*] Yongzhe Guo,[1] Zhengzhi Wang,[1,2,*] Steven O. Nielsen,[3] and Ray H. Baughman[3,4,*]

SUMMARY

The strength and toughness of materials are important for applications. A linear atomic chain, carbyne, has been previously predicted to have the highest strength and toughness. To discover materials with higher gravimetric strength and toughness, we herein investigated B, C, N, BC, BN, and CN chains by first-principles calculations. We found that B, C, BC, and BN chains are stable when under tension at room temperature. B chains have the highest recorded gravimetric toughness (16.9 kJ g^{-1}), whereas BC chains have the highest recorded gravimetric strength (91.8 GPa g^{-1} cm^3) and high toughness (15.3 kJ g^{-1}), surpassing the predicted performance of carbyne (76.4 GPa g^{-1} cm^3 and 9.4 kJ g^{-1}). Electronic structure analyses show that the higher strength and toughness of the BC and B chains, compared with carbyne, originate from their strong chemical bonding and the absence of a Peierls instability up to strain to failure. The potential fabrication and applications of BC and B chains are discussed.

INTRODUCTION

Linear atomic chains possess extreme properties as a result of their unusual structures.[1–4] Considerable effort has been devoted to the prediction and discovery of linear atomic chains,[5–7] such as H chains,[8] B chains,[9] C chains,[4,10–12] P chains,[13] Au chains,[14] and BN chains.[15,16] Because of their low coordination and ultrahigh specific surface area, linear atomic chains usually exhibit a higher energy above hull than other allotropes. For example, some materials containing linear carbon chains even explode.[5,17,18] Hence, the existence of atomic chains has long been questioned. Fortunately, a few methods for the fabrication of atomic chains have been recently developed, including the following: (1) making atomic chains from other allotropes, for example, deriving carbon chains from graphene[10] and BN chains from *h*-BN[15]; (2) synthesizing atomic chains from chemical sources, for example, the synthesis of carbon chains.[19,20] Because of their high energy above hull, it is sometimes challenging to stabilize atomic chains. To this end, facile techniques have been developed, such as mechanically deriving linear chains from other phases,[10] using end-capping groups for stabilization,[20–22] and using carbon nanotubes (CNTs) as a confining host.[12,19,23] For instance, Chalifoux and Tykwinski[20] have synthesized carbon chains containing 44 carbon atoms by capping these chains with bulky end groups. Shi et al.[19] have synthesized the longest presently reported carbon chain (containing > 6,000 atoms) inside a double-walled nanotube, demonstrating that long atomic chains can be fabricated in protected environments.

Atomic chains can be used for angstrom-scale devices[7,24] and macroscopic fiber assemblies.[3] The strength and toughness of atomic chains are important for their use in practical applications.[4,10,13] The reported strength for many types of atomic chains is

Progress and potential

Carbyne, a linear atomic chain, has been predicted to have the highest strength and toughness. In this work, we explored potential high-strength and high-toughness atomic chains by first-principles calculations. Our calculations indicated that linear B, C, BC, and BN chains are stable during stretching at room temperature. Linear BC chains have a higher predicted gravimetric strength than carbyne, and the predicted gravimetric toughnesses of linear B and BC chains are much higher than calculated for carbyne. To our knowledge, no other materials have been found to have a higher gravimetric strength than linear BC chains and a higher gravimetric toughness than linear BC and B chains. The underlying mechanism for the high strength and toughness of BC and B chains is from their strong bonding and the absent Peierls instability up to strain to failure.

controversial, mainly because of variations in the reported cross-sectional areas. For example, when the cross-sectional area of carbon chains is adopted as 0.468, 3.14, and 11.22 $Å^2$, the theoretical values of the tensile strength become 2,501, 373, and 104 GPa, respectively.[4] To avoid controversies regarding the cross-sectional area, gravimetric strength (the breaking force divided by the linear mass density) is a less controversial measure for the strength of atomic chains. Hence, we use gravimetric strength as the metric for measuring the strength. Also, we use gravimetric toughness as the metric for measuring the toughness. Linear C chains have two possible structures [(=C=C=) and (–C≡C–)]. According to Peierls theorem, a linear metallic monoatomic chain with one delocalized electron per atom should dimerize and thereby convert to an insulator. Literature results show that linear C chains exhibit dimerization, which is attributed to Peierls theorem.[25] Herein, we call these linear C chains "carbyne." Carbyne has been predicted to have the highest gravimetric strength and gravimetric toughness (76.4 GPa g^{-1} cm^3 and 9.4 kJ g^{-1}, respectively), even greater than such materials as diamond, CNTs, and graphene.[3,4,26] However, because of the Peierls instability, carbyne contains alternating strong triple bonds and weak single bonds. The mechanical strength and toughness of carbyne are reduced because of an increased degree of bond alternation between single and triple bonds during stretching, as chain rupture occurs at the longest and weakest bond. Therefore, it remains to be determined if other atomic chains exist that are free of a Peierls instability for all accessible tensile strains and thus perhaps have a higher strength and toughness than carbyne.

Because B, C, and N can form high-modulus, high-strength materials (such as diamond and the wurtzite phase of boron nitride)[27] and these elements are lightweight and have small covalent radii, we investigated the B, C, N, BC, BN, and CN chains illustrated in Figure 1A. First-principles calculations show that there is a significant energy barrier for converting linear B, C, BC, and BN chains to other materials, indicating their metastability. These calculations indicate that the strain to failure of the BC and B chains (25% and 31%, respectively) are much larger than for C chains (18%). Herein, the strain to failure is defined as the strain corresponding to the maximum stress. Most interestingly, the linear BC chain has a higher gravimetric strength (91.8 GPa g^{-1} cm^3) and toughness (15.3 kJ g^{-1}), while the B chain has a higher gravimetric toughness (16.9 kJ g^{-1}) than carbyne (76.4 GPa g^{-1} cm^3 and 9.4 kJ g^{-1}), which holds the previous record for the highest gravimetric strength and highest gravimetric toughness material. The main reason for this higher gravimetric strength and toughness is that the Peierls instability observed for linear C chains does not occur for linear BC and B chains, even when these chains are stretched to failure. Finally, the possible fabrication and applications of BC and B chains are discussed.

RESULTS AND DISCUSSION

Computations for linear atomic chains

Density-functional theory (DFT) calculations were first used to establish whether or not linear B, C, N, BC, BN, and CN chains (Figure 1A) are internally dimerized, which means that they form an alternating bond structure. Such dimerization has been well established for a linear C chain, indicating that the cumulene structure (=C=C=) with consecutive double bonds is less stable than the polyyne structure (–C≡C–) with alternating single and triple bonds.[28] Our calculations confirm this instability of a linear C chain by showing the bond alternation of the polyyne structure. However, DFT calculations using the hybrid HSE06 functional show that linear B, N, BC, BN, and CN chains have uniform bond lengths of 1.55, 1.25, 1.39, 1.30, and 1.22 Å, respectively. Consequently, these non-stretched chains are free of Peierls distortion.

[1]Department of Engineering Mechanics, School of Civil Engineering, Wuhan University, Wuhan, Hubei 430072, China

[2]State Key Laboratory of Water Resources and Hydropower Engineering Science, Wuhan University, Wuhan, Hubei 430072, China

[3]Department of Chemistry and Biochemistry, The University of Texas at Dallas, Richardson, TX 75080, USA

[4]Alan G. MacDiarmid NanoTech Institute, The University of Texas at Dallas, Richardson, TX 75080, USA

[5]Lead contact

*Correspondence: enlaigao@whu.edu.cn (E.G.), zhengzhi.wang@whu.edu.cn (Z.W.), ray.baughman@utdallas.edu (R.H.B.)

https://doi.org/10.1016/j.matt.2022.01.021

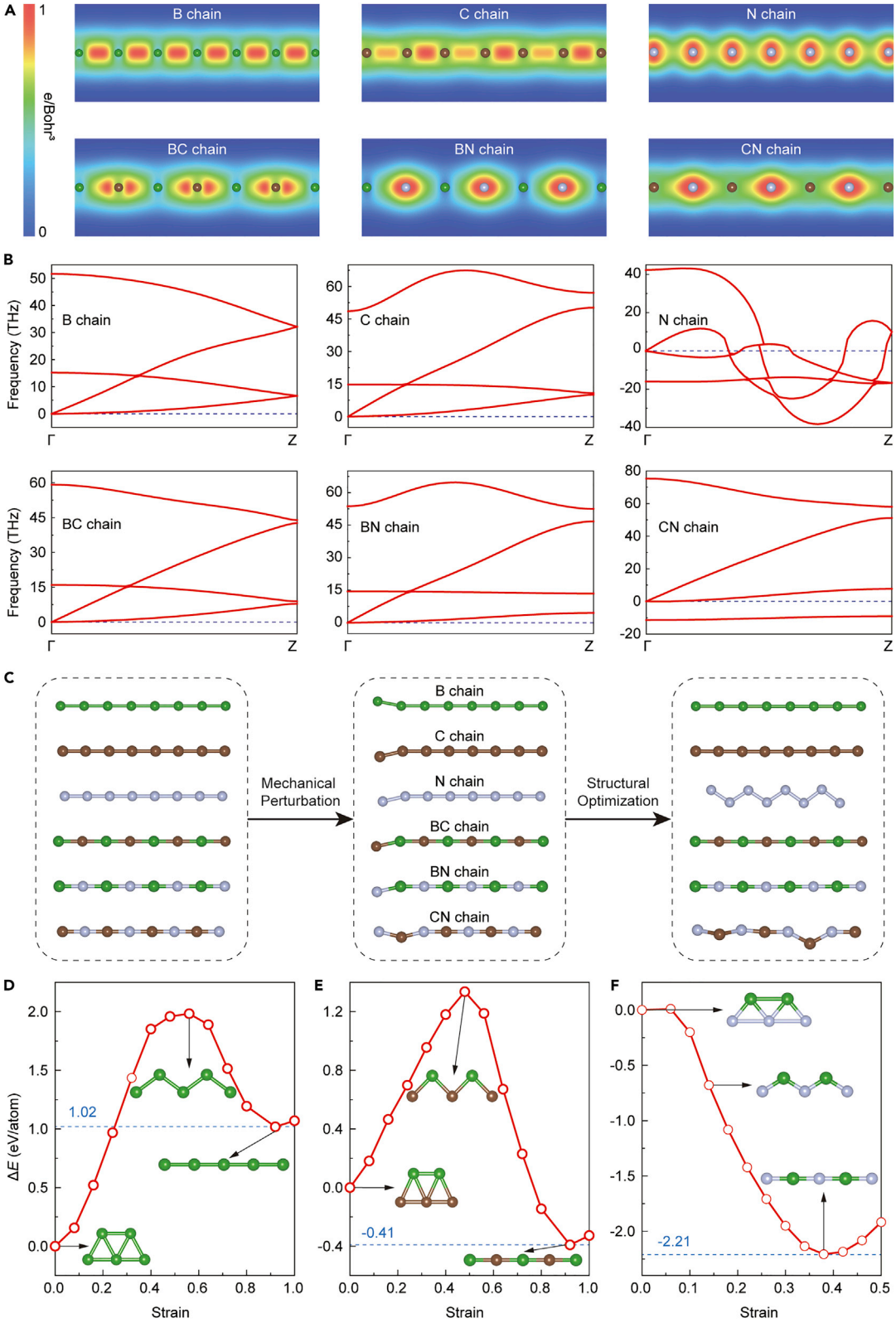
A
1
e/Bohr³
0
B chain
C chain
N chain
BC chain
BN chain
CN chain
B
Frequency (THz)
Γ
Z
C
Mechanical Perturbation
Structural Optimization
D
E
F
ΔE (eV/atom)
Strain
1.02
-0.41
-2.21

Figure 1. Structures and stabilities of linear atomic chains
(A) Charge density distribution for linear B, C, N, BC, BN, and CN chains.
(B) Phonon dispersion curves of linear B, C, N, BC, BN, and CN chains.
(C) Linear B, C, N, BC, BN, and CN chains under mechanical perturbation. Only the N and CN chains are unstable with respect to perturbations from linearity.
(D–F) Phase transitions between linear chains and ribbon-like chains, in which the energy change as a function of strain are shown for B (D), BC (E), and BN (F) chains.

Previous calculations for B and BN chains support these results of equidistant bonds and agree in the predicted bond lengths for these chains (1.55 and 1.30 Å, respectively).[9,29] As shown in the following discussion, our calculations additionally indicate that the absence of bond alternation for linear B, BC, and BN chains persists up to chain fracture, while linear N and CN chains are unstable.

Stabilities of linear atomic chains

Phonon calculations provide a criterion for quantifying structural stability. Our calculations do not find negative frequencies, i.e., imaginary frequencies in the phonon dispersion curves for linear B, C, BC, and BN chains (Figure 1B), which indicates their dynamic stabilities. However, there are imaginary modes for linear N and CN chains, indicating that N and CN chains do not have energy minima. To confirm this, a mechanical perturbation, consisting of a random displacement of any one atom by 0.3 Å from its energy-minimized position, was applied to these atomic chains. Thereafter, the perturbed structures were re-optimized by energy minimization. These calculations show that the linear N and CN chains are not stable with respect to distortions from linearity, even at 0 K (Figure 1C). However, B, C, BC, and BN chains recover from the perturbation, indicating that the linear chain is an equilibrium structure. The thermodynamic stability of linear B, C, N, BC, BN, and CN chains in a supercell (12 atoms) was further evaluated by *ab initio* molecular dynamics (AIMD) simulations for 10 ps at 300 K. The temperature was controlled by using a Nosé-Hoover thermostat. During the AIMD simulations, B, C, BC, BN, and CN chains upheld their structural integrity with only slight corrugation owing to thermal fluctuations, while the N chain decomposed into short segments and N_2 molecules (see Figure S1 and Video S1 for details). Considering the instability of linear N and CN chains, only B, C, BC, and BN chains are further discussed. To further address thermodynamic stability, we performed AIMD simulations of finite-length B, C, BC, and BN chains for 10 ps at 300 K without periodic boundaries and without tension. These finite-length chains with hydrogen termination maintain structural integrity for the duration of the simulations (Video S2).

Cohesive energy provides a useful criterion for characterizing the bonding and thermal stability of atomic chains. Herein, the cohesive energy is defined as the difference between the energy of the isolated atoms and the corresponding atomic chains (normalized per atom). The calculated cohesive energies of B, C, BC, and BN chains are 4.75, 6.99, 6.03, and 6.29 eV/atom, respectively, which shows that these linear chains are strongly bonded. In agreement with our predictions on the stabilities of linear B, C, and BN chains, linear C and BN chains or segments have been observed,[10,12,15,19,20] and linear B, C, and BN chains have been predicted.[4,9]

Additionally, Yakobson's group has shown that a linear B chain has a higher energy than a ribbon-like chain and that the ribbon-like B chain can transform to a linear B chain for tensile strains above 92%.[9] Our calculations confirm the higher energy of the linear B chain and the mechanically driven transition between the ribbon-like B chain and the linear B chain (Figure 1D). However, for BC and BN chains, our calculations show that the ribbon-like chain has a higher energy than the linear chain for all

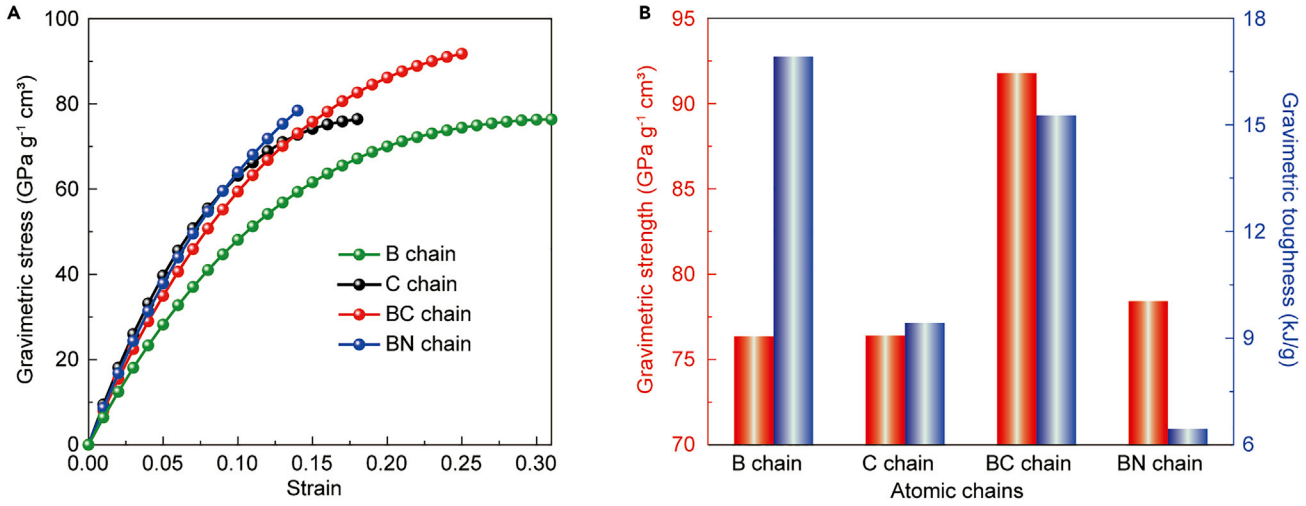

Figure 2. Mechanical properties of linear atomic chains

(A and B) Gravimetric stress-strain curves (A) and gravimetric strength and gravimetric toughness (B) of B, C, BC, and BN chains, obtained from DFT calculations using the HSE06 functional.

tensile strains (Figures 1E and 1F). For C chains, such ribbon-like configuration is not even an energy minimum.

Mechanics of linear atomic chains

We performed tensile tests and calculated the gravimetric stress-strain curves for B, C, BC, and BN chains by using the DFT method (Figure 2). These DFT calculations were conducted using the local density approximation (LDA), the generalized gradient approximation (GGA), and the hybrid HSE06 functional incorporating exact exchange (the most trustworthy, yet most costly method). As shown in Figure S2, calculations on gravimetric stress versus strain curves for linear chains as a function of strain using these methods are in good agreement. Considering the accuracy, the below-reported tensile mechanical properties and the relevant structural analyses were calculated at the hybrid HSE06 functional level. The thereby calculated gravimetric moduli of the BN and carbyne chains (868 and 945 GPa g^{-1} cm^3, respectively) agree with values (862 and 982 GPa g^{-1} cm^3, respectively) calculated using literature-reported chain force constants[30] and the linear mass densities of these chains. These results show that linear B, BC, and BN chains have a lower gravimetric modulus (643, 802, and 868 GPa g^{-1} cm^3, respectively) than carbyne (945 GPa g^{-1} cm^3).

The bending stiffness (k_b) was also calculated from the energy (E_b) required to bend an arbitrarily long linear atomic chain into a circle with radius R: $k_b = 2(E_b/L)/q^2$, where $L = 2\pi R$ and $q = 1/R$ are the circumference and curvature of the circle, respectively. Thus, $k_b = E_b R/\pi$. The thereby calculated bending stiffnesses for linear B, C, BC, and BN chains were 1.7, 3.7, 1.8, and 1.3 eV Å, respectively (see the bending configurations of these chains in Figure S3). These chains will behave like a rigid rod at temperature T for chain lengths shorter than the persistence length ($l_p = k_b/kT$, where k is the Boltzmann constant). At room temperature, the persistence lengths of the linear B, C, BC, and BN chains are 6.6, 14.2, 7.0, and 5.0 nm, respectively. Hence, the bending flexibilities are in the following order: BN > B > BC > C.

The calculated gravimetric strength of carbyne (76.4 GPa g^{-1} cm^3) is close to the value (71.1 GPa g^{-1} cm^3) obtained by dividing the experimentally determined

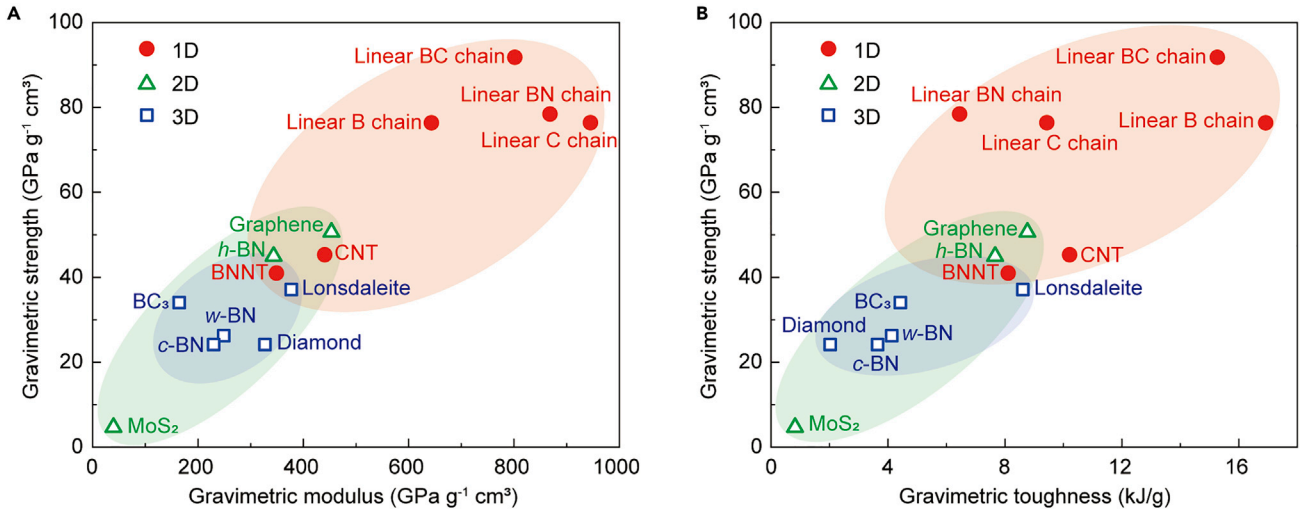

Figure 3. Calculated modulus, strength, and toughness

(A and B) Gravimetric strength versus gravimetric modulus (A) and gravimetric strength versus gravimetric toughness (B) for high mechanical performance materials. The data can be found in Table S1.

breaking force of 11.1 nN[31] by the calculated weight per length for a single carbon chain. Surprisingly, the BC chain has a significantly higher gravimetric strength (91.8 GPa g^{-1} cm^3) than carbyne (76.4 GPa g^{-1} cm^3), which holds the previous record as the highest gravimetric strength material. This higher gravimetric strength mainly results from the much higher strain to failure of BC chain (25%) than for carbyne (18%) (Figure 2). To our knowledge, the gravimetric strength of this chain is higher than for any other material (Figure 3 and Table S1). For example, the gravimetric strengths of graphene and diamond are only 50.6 and 24.2 GPa g^{-1} cm^3, respectively. Confidence in these relative results for different materials is increased by the fact that the same computational method was employed and that agreement was found with literature results for the gravimetric modulus and gravimetric strength of C chains.[4] Also, the phonon spectra indicate the dynamic stability of these chains even near their strains to failure (Figure S4).

Moreover, the linear B and BC chains have the highest predicted gravimetric toughnesses (16.9 and 15.3 kJ g^{-1}, respectively), which are much higher than for carbyne (9.4 kJ g^{-1}). In fact, these predicted toughnesses for B and BC chains are at least ~1.5 times higher than previously predicted for any material. For comparison, the measured gravimetric toughness for the Kevlar fibers used for antiballistic vests is only 0.078 kJ g^{-1}.[32] Furthermore, in contrast to other super-tough materials, the energy is absorbed elastically by the linear B and BC chains, so these linear fibers are not damaged before fracture.

In addition to the above-mentioned binary linear chains, namely $(\text{-B-C-})_n$ and $(\text{-B-N-})_n$, we also explored the mechanical behavior for other possible linear chains with these compositions (Figure S5), such as $(\text{-B-B-C-C-})_n$ and $(\text{-B-B-N-N-})_n$. However, the gravimetric strength (69.6 and 47.8 GPa g^{-1} cm^3, respectively) and gravimetric toughness (7.6 and 5.0 kJ g^{-1}, respectively) of $(\text{-B-B-C-C-})_n$ and $(\text{-B-B-N-N-})_n$ chains are much lower than for $(\text{-B-C-})_n$ and $(\text{-B-N-})_n$ chains, as each of these longer period chains have three types of bonds, and one bond is weaker than the others, which is where failure occurs. The failure occurs at the B-B bond for both the $(\text{-B-B-C-C-})_n$ and the $(\text{-B-B-N-N-})_n$ chains. These results establish that structures

possessing uniform bonds have enhanced mechanical properties, as there is no weakest link.

Mechanism for the ultrahigh strength and toughness of B and BC chains

To understand the ultrahigh strength of the B and BC chains, the bond structure and its dependence on the applied tensile strain were calculated based on the electron density distribution. Carbyne suffers from a Peierls instability, and the bond alternation increases with increasing tensile strain.[4] Because the strength of linear atomic chains is determined by the weakest chemical bond, the tensile strength of carbyne is reduced by these issues. In the following discussion, the criteria used for measuring the Peierls distortion includes the bond length alternation and the bond order alternation of linear atomic chains. If these alternations are zero, it is concluded that the Peierls distortion is absent.

To quantify the bonding of linear B and BC chains, the charge transfer between neighboring atoms in these chains was calculated by using Bader's atoms-in-molecules approach.[33] In the Bader charge calculations, the atomic charge includes the charge in neighboring bonds that is associated with the atom. The obtained results show that the charge transfer between neighboring atoms in linear B and BC chains are 0.00 *e* and 1.90 *e*, respectively, while this charge-transfer is near zero for linear C chains. Meanwhile, the neighboring bond orders (the number of chemical bonds between a pair of atoms) for linear B, C, and BC chains are calculated as 1.60/1.60, 1.86/2.35, and 1.75/1.75, respectively, based on a refinement of the density-derived electrostatic and chemical approach.[34] The results for the linear C chains indicate the existence of a Peierls instability, while no bond alternation exists for the linear B and BC chains (Figure 4A). These results agree with previous calculations showing the bond alternation in linear C chains.[4] To summarize, the large charge-transfer and large bond order predicted for the linear BC chain indicate its strong polar covalent bonding, while the zero charge-transfer and large bond order predicted for the linear B chain indicate its strong covalent bonding.

The dependence of bond lengths and bond orders on tensile strain were calculated for these linear chains. These results show that for all tensile strains up to failure, there is only one uniform bond for B and BC chains, while the bond alternation increases for linear C chains with increasing tensile strain (Figures 4B and 4C). Interestingly, Cab et al.[30] have predicted that the bond alternation in linear C chains vanishes on uniaxial compression strain of about 3%. The uniform bonding for linear B and BC chains indicates the absence of a Peierls instability under tension. Moreover, the bond order decreases with increasing tensile strain. The bond orders of neighboring bonds for strain-free carbyne chains were both greater than those for strain-free B and BC chains, while the bond order of the long bond in carbyne decreases and the bond order of the short bond generally increases with increasing strain. For tensile strains above 8% and 4%, respectively, the bond orders in B and BC chains exceed the bond order of the long bond in carbyne (Figure 4B). Also, the bond order alteration and the bond length alternation in carbyne increases with increasing strain (Figures 4B, 4C, and S6), largely because of the length increase of the long bond. The strain dependence of the electron densities further supports the absence of a Peierls instability for linear B and BC chains under tension before strain to failure (Figure 4D). To further explore the bond alternation of linear B, C, and BC chains, we investigated their energy differences under strain to failure and a strain 1% higher than the strain to failure as a function of the bond length alternation (Figure 5). Compared with the alternating bond structures that are energy

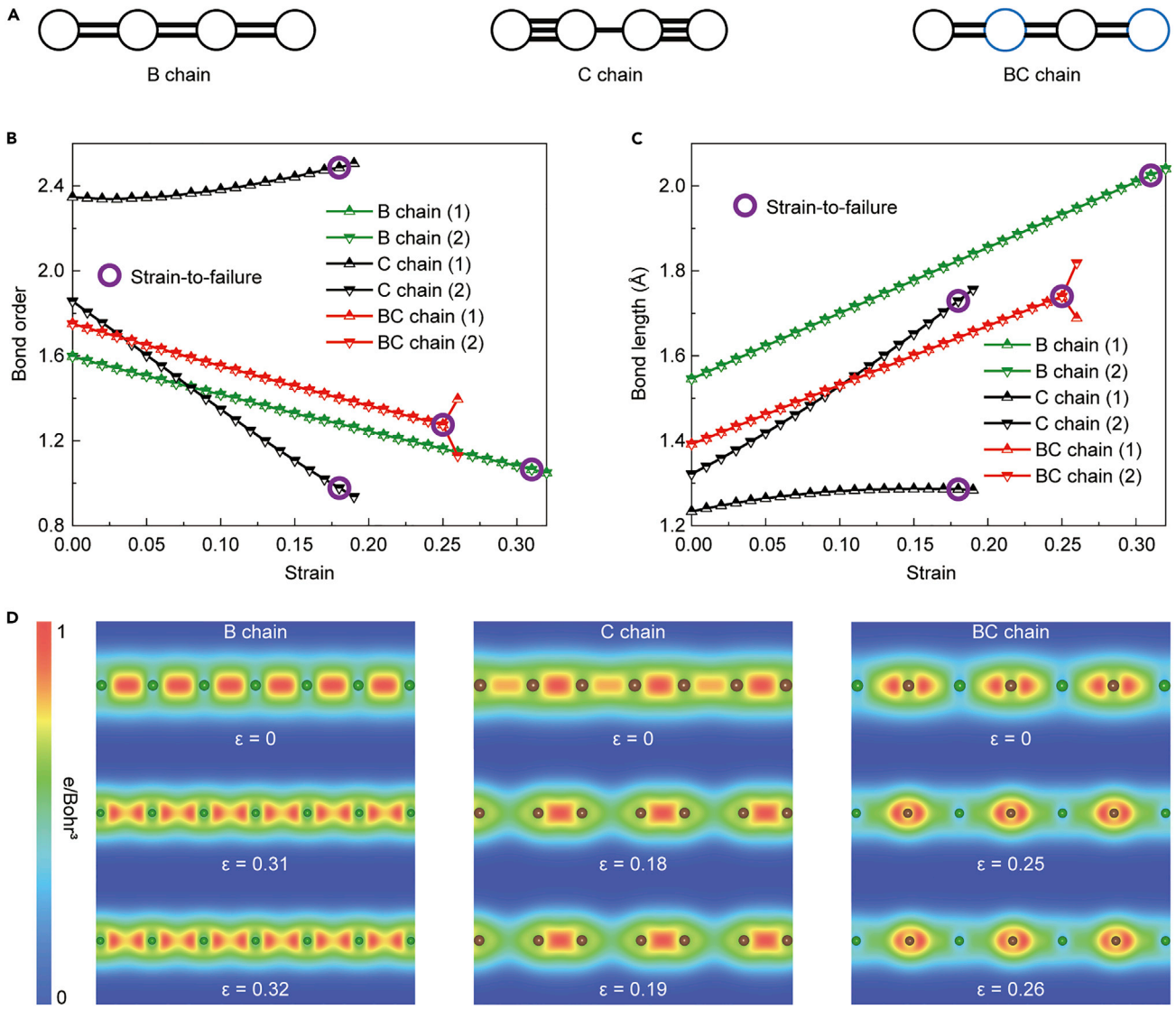

Figure 4. Atomic and electronic structures of B, C, and BC chains

(A) Schematic diagrams of linear B, C, and BC chains.

(B and C) Bond order (B) and bond length (C) of neighboring bonds in B, C, and BC chains as a function of tensile strain. The strain-to-failure points are marked with purple circles.

(D) Charge density distribution for linear B, C, and BC chains under zero strain, strain to failure, and a strain 1% higher than the strain to failure.

minima for linear C chains both before and after strain to failure, the energy minima correspond to uniform bond configurations until strain to failure for BC chain and even just after strain to failure for B chain. It should be noted here that the energy difference between alternating bonding and uniform bonding phases for linear B, C, and BC chains near the strain-to-failure transition is extremely small (Figure 5). Hence, additional convergence tests were performed, and stringent convergence criteria were adopted to correctly capture this behavior (see experimental procedures for details). In summary, the strong bonding and the resistance to Peierls instability for linear B and BC chains up to their large strains to failure endow them with exceptional gravimetric strength and toughness.

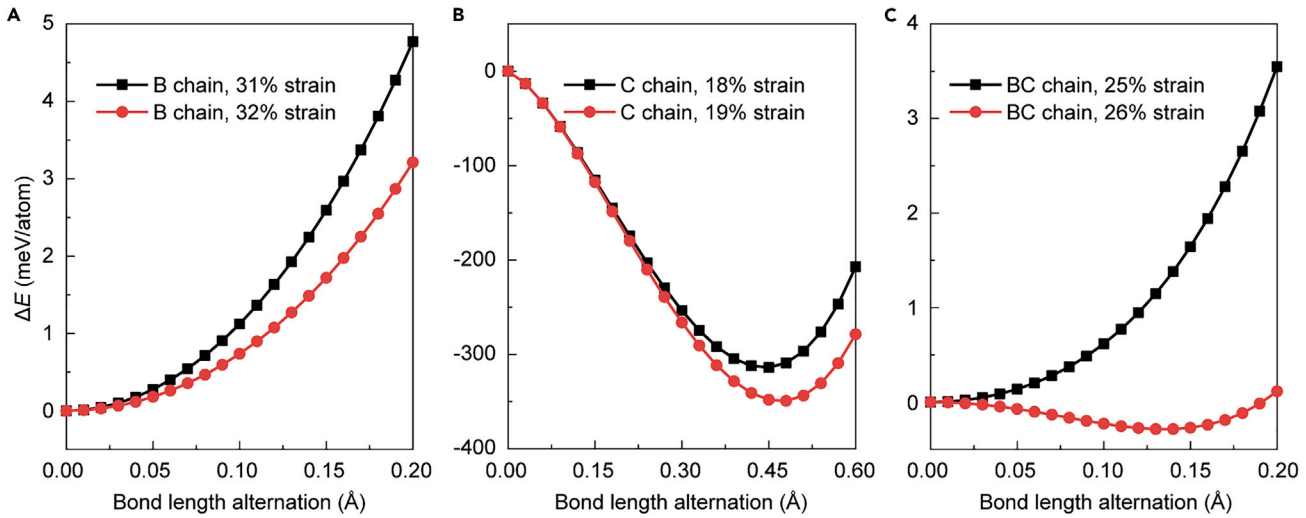

Figure 5. Energies of linear B, C, and BC chains near the strain to failure

(A–C) Energy differences between alternating bonding and uniform bonding of linear B (A), C (B), and BC (C) chains under strain to failure (black squares) and a strain 1% higher than the strain to failure (red circles) as a function of bond length alternation.

Possible synthesis methods

Formability and stability are critical for determining whether atomic chains can be used. For characterizing these aspects, we calculated the energy above hull. This is the energy difference at zero pressure and zero temperature between the energy for an isolated linear chain and that of the lowest energy material having the same overall chemical composition. Herein, the calculated energy above hull of linear B, C, and BC chains are 1.77, 1.03, and 1.31 eV/atom, respectively. This suggests that the likely ease of chain fabrication can be sequenced as C > BC > B.

As linear C and BN chains have been fabricated by drawing these chains from a 2D sheet of graphene[10] and BN,[15] respectively, we first considered this approach for the possible synthesis of linear B and BC chains. Considering that 2D phases of boron have been predicted and successfully fabricated,[35] it is promising to derive boron atomic chains from these planar boron structures. However, the known 2D phase of boron carbide is a planar BC_3 sheet,[36] in which each carbon atom is in a hexagonal C_6 ring and each C has only one neighboring B. Hence, a linear BC chain cannot be formed by solely breaking bonds in this planar structure. On the other hand, the fabrication of linear B and BC chains within carbon nanotubes might be possible, just as it has been possible to fabricate many other materials within the hollow core of carbon nanotubes, including metal nanowires.[37–40] It might even be possible to obtain linear B and BC chains within carbon nanotubes by using the carbon-arc methods that have been used to form carbyne chains inside carbon nanotubes. Instead of using carbon electrodes for producing the carbon arc, the electrodes would comprise boron for B chains and a compacted mixture of boron and BC_3 sheets for BC chains.

To modify the properties for applications, segments of different chain types could be combined in the same chain, or bundles could be made using chains of different types. In fact, previous work has demonstrated that heterochains of C and BN exhibit tunable electronic transport properties.[41] As linear chains can form bundles or crystals through inter-chain van der Waals interactions, as is the case for carbyne crystals,[42,43] the stability of linear atomic chains with respect to inter-chain reactions is important. For example, the reaction of arrays of carbyne chains can be

explosive.[5,17,18] Also, cross-linking between two carbyne chains by forming four-membered rings is known, as is the 1,4-addition polymerization of arrays of carbyne chain segments.[6,44] However, inter-chain reactions of linear B and BC chains have not yet been investigated. Guided by experimental evidence for the formation of four-membered rings for linear C chains,[4,45] we modeled the formation of such rings as a representative inter-chain crosslinking reaction. These calculations indicate that parallel B chains react to produce a ribbon structure that does not contain four-membered rings. Figure S7 shows the DFT-calculated reaction energy per ring as a function of the separation between reacting atoms for the formation of a four-membered ring by crosslinking linear C and BC chains. The system energy change for the formation of one four-membered ring is −0.37 and −1.08 eV for linear C and BC chains, respectively, indicating that these reactions are thermodynamically favorable. However, the kinetic energy barriers for these inter-chain reactions are significant, indicating the kinetic stability of these chains for this reaction in the absence of applied stresses. These results generally suggest that attention should be paid to possible inter-chain reactions during the synthesis of these chains. Previous developed techniques for preventing inter-chain reactions of linear C chains, such as pre-stretching linear chains,[10] using end-capping groups for isolation,[20–22] and using CNTs as a confining host,[12,19,23] could be considered for the stabilization of chain bundles. For example, our previous study demonstrated that a bundle of linear C chains confined within a CNT exhibits confinement-enhanced stability.[3]

Conclusions

In this study, we predicted the properties of B, C, N, BC, BN, and CN linear atomic chains by first-principles calculations. From the phonon spectra and the response to mechanical perturbations, we showed that linear N and CN chains are not stable. Linear C chains have a Peierls instability that is amplified with increasing tension. In contrast, we showed that the bonds in linear B and BC chains remain equivalent for all tensile strains up to failure, indicating the complete absence of a Peierls instability. Our calculations predict that linear BC chains have a higher gravimetric strength (91.8 GPa g^{-1} cm^3) than carbyne (76.4 GPa g^{-1} cm^3), which was the previously reported highest strength material. Most interestingly, the predicted gravimetric toughnesses of linear B (16.9 kJ g^{-1}) and BC (15.3 kJ g^{-1}) chains are much higher than calculated for carbyne (9.4 kJ g^{-1}). To our knowledge, no other materials have been predicted or experimentally found to have a higher gravimetric strength than linear BC chains and a higher gravimetric toughness than linear BC and B chains.

EXPERIMENTAL PROCEDURES

Resource availability

Lead contact

Further information and requests for resources and materials should be directed to and will be fulfilled by the lead contact, Enlai Gao (enlaigao@whu.edu.cn).

Materials availability

This study did not generate any reagents.

Data and code availability

All data and codes in the article are available upon reasonable request to the lead contact.

First-principles calculations

To investigate the stabilities, formability, and mechanical properties of atomic chains, first-principles calculations based on the density functional theory (DFT)

framework were performed by using the Vienna *Ab-Initio* Simulation Package (VASP).[46] Unless otherwise noted, the Perdew-Burke-Ernzerhof parameterization[47] of the generalized gradient approximation was used for the exchange-correlation functional. For higher accuracy, the tensile mechanical properties and the relevant structural analyses were calculated at the hybrid HSE06 functional level. Projector augmented wave potentials were used to treat ion-electron interactions.[48] An energy cutoff of 1.3 times the default value was used, and a *k*-point mesh with a density of about 75 Å (the product of each lattice constant and the corresponding number of *k*-points) was used for Brillouin zone sampling.[49] The conjugate gradient algorithm was adopted for geometry relaxation, in which the energy and the forces on atoms are converged to below 5×10^{-2} meV/atom and 5×10^{-3} eV/Å, respectively, unless otherwise noted. The energy difference between alternating bond and uniform bond geometries for linear B, BC, and BN chains near the strain-to-failure is very small. Hence, additional energy convergence tests were performed, and more stringent convergence criteria of the energy (5×10^{-6} meV/atom) and the forces on atoms (5×10^{-6} eV/Å) were adopted to ensure accurate results. A 20 Å vacuum layer was used in the aperiodic directions and held constant through modifying the VASP code to minimize the interaction between periodic images.

SUPPLEMENTAL INFORMATION

Supplemental information can be found online at https://doi.org/10.1016/j.matt.2022.01.021.

ACKNOWLEDGMENTS

This work in China was supported by the National Natural Science Foundation of China (12172261, 11902225 and 11972264). This work in the United States was supported by the Robert A. Welch Foundation (grant AT-0029). The numerical calculations in this work have been performed on a supercomputing system in the Supercomputing Center of Wuhan University. We acknowledge Prof. Baoshan Wang of Wuhan University for helpful discussions.

AUTHOR CONTRIBUTIONS

R.H.B. and E.G. conceived the idea. E.G. and Y.G. conducted the simulations. E.G., Z.W., S.O.N., and R.H.B. contributed to data analysis, scientific discussion, and the writing of the manuscript.

DECLARATION OF INTERESTS

The authors declare no competing interests.

Received: October 21, 2021
Revised: December 22, 2021
Accepted: January 26, 2022
Published: February 16, 2022

REFERENCES

1. Shi, L., Senga, R., Suenaga, K., Kataura, H., Saito, T., Paz, A.P., Rubio, A., Ayala, P., and Pichler, T. (2021). Toward confined carbyne with tailored properties. Nano Lett. *21*, 1096–1101.

2. Naden Robinson, V., Zong, H., Ackland, G.J., Woolman, G., and Hermann, A. (2019). On the chain-melted phase of matter. Proc. Natl. Acad. Sci. U S A *116*, 10297–10302.

3. Gao, E., Li, R., and Baughman, R.H. (2020). Predicted confinement-enhanced stability and extraordinary mechanical properties for carbon nanotube wrapped chains of linear carbon. ACS Nano *14*, 17071–17079.

4. Liu, M., Artyukhov, V.I., Lee, H., Xu, F., and Yakobson, B.I. (2013). Carbyne from first principles: chain of C atoms, a nanorod or a nanorope. ACS Nano *7*, 10075–10082.

5. Baughman, R.H. (2006). Dangerously seeking linear carbon. Science *312*, 1009–1110.

6. Baughman, R.H., and Yee, K.C. (1978). Solid-state polymerization of linear and cyclic acetylenes. J. Polym. Sci. Part A. *13*, 219–239.

7. Agrait, N., Yeyati, A.L., and van Ruitenbeek, J.M. (2003). Quantum properties of atomic-sized conductors. Phys. Rep. *377*, 81–279.

8. Motta, M., Genovese, C., Ma, F.J., Cui, Z.H., Sawaya, R., Chan, G.K.L., Chepiga, N., Helms, P., Jimenez-Hoyos, C., Millis, A.J., et al. (2020). Ground-state properties of the hydrogen chain: dimerization, insulator-to-metal transition, and magnetic phases. Phys. Rev. X *10*, 031058.

9. Liu, M., Artyukhov, V.I., and Yakobson, B.I. (2017). Mechanochemistry of one-dimensional boron: structural and electronic transitions. J. Am. Chem. Soc. *139*, 2111–2117.

10. Jin, C., Lan, H., Peng, L., Suenaga, K., and Iijima, S. (2009). Deriving carbon atomic chains from graphene. Phys. Rev. Lett. *102*, 205501.

11. Artyukhov, V.I., Liu, M., and Yakobson, B.I. (2014). Mechanically induced metal-insulator transition in carbyne. Nano Lett. *14*, 4224–4229.

12. Zhao, X., Ando, Y., Liu, Y., Jinno, M., and Suzuki, T. (2003). Carbon nanowire made of a long linear carbon chain inserted inside a multiwalled carbon nanotube. Phys. Rev. Lett. *90*, 187401.

13. Xiao, Z.R., Qiao, J.S., Lu, W.L., Ye, G.J., Chen, X.H., Zhang, Z., Ji, W., Li, J.X., and Jin, C.H. (2017). Deriving phosphorus atomic chains from few-layer black phosphorus. Nano Res. *10*, 2519–2526.

14. Okamoto, M., and Takayanagi, K. (1999). Structure and conductance of a gold atomic chain. Phys. Rev. B *60*, 7808–7811.

15. Cretu, O., Komsa, H.P., Lehtinen, O., Algara-Siller, G., Kaiser, U., Suenaga, K., and Krasheninnikov, A.V. (2014). Experimental observation of boron nitride chains. ACS Nano *8*, 11950–11957.

16. Arenal, R., and Lopez-Bezanilla, A. (2015). Boron nitride materials: an overview from 0D to 3D (nano)structures. Wiley Interdiscip. Rev. *5*, 299–309.

17. Tykwinski, R.R., Chalifoux, W., Eisler, S., Lucotti, A., Tommasini, M., Fazzi, D., Del Zoppo, M., and Zerbi, G. (2010). Toward carbyne: synthesis and stability of really long polyynes. Pure Appl. Chem. *82*, 891–904.

18. Prenzel, D., Kirschbaum, R.W., Chalifoux, W.A., McDonald, R., Ferguson, M.J., Drewello, T., and Tykwinski, R.R. (2017). Polymerization of acetylene: polyynes, but not carbyne. Org. Chem. Front. *4*, 668–674.

19. Shi, L., Rohringer, P., Suenaga, K., Niimi, Y., Kotakoski, J., Meyer, J.C., Peterlik, H., Wanko, M., Cahangirov, S., Rubio, A., et al. (2016). Confined linear carbon chains as a route to bulk carbyne. Nat. Mater. *15*, 634–639.

20. Chalifoux, W.A., and Tykwinski, R.R. (2010). Synthesis of polyynes to model the *sp*-carbon allotrope carbyne. Nat. Chem. *2*, 967–971.

21. Johnson, T.R., and Walton, D.R.M. (1972). Silylation as a protective method in acetylene chemistry. Tetrahedron *28*, 5221–5236.

22. Gibtner, T., Hampel, F., Gisselbrecht, J.P., and Hirsch, A. (2002). End-cap stabilized oligoynes: model compounds for the linear *sp* carbon allotrope carbyne. Chem. Eur. J. *8*, 408–432.

23. Nishide, D., Dohi, H., Wakabayashi, T., Nishibori, E., Aoyagi, S., Ishida, M., Kikuchi, S., Kitaura, R., Sugai, T., Sakata, M., and Shinohara, H. (2006). Single-wall carbon nanotubes encaging linear chain $C_{10}H_2$ polyyne molecules inside. Chem. Phys. Lett. *428*, 356–360.

24. Cui, L., Jeong, W., Hur, S., Matt, M., Klockner, J.C., Pauly, F., Nielaba, P., Cuevas, J.C., Meyhofer, E., and Reddy, P. (2017). Quantized thermal transport in single-atom junctions. Science *355*, 1192–1195.

25. Kartoon, D., Argaman, U., and Makov, G. (2018). Driving forces behind the distortion of one-dimensional monatomic chains: Peierls theorem revisited. Phys. Rev. B *98*, 165429.

26. Zhang, K., Zhang, Y.F., and Shi, L. (2020). A review of linear carbon chains. Chin. Chem. Lett. *31*, 1746–1756.

27. Pan, Z., Sun, H., Zhang, Y., and Chen, C. (2009). Harder than diamond: Superior indentation strength of wurtzite BN and lonsdaleite. Phys. Rev. Lett. *102*, 055503.

28. Kertesz, M., Koller, J., and Aman, A. (1978). Ab initio Hartree–Fock crystal orbital studies. II. Energy bands of an infinite carbon chain. J. Chem. Phys. *68*, 2779.

29. Abdurahman, A., Shukla, A., and Dolg, M. (2002). Ab initio many-body calculations on infinite carbon and boron-nitrogen chains. Phys. Rev. B *65*, 115106.

30. Cab, C., Medina, J., Casais-Molina, M.L., Canto, G., and Tapia, A. (2019). Ultrahigh stretching bond force constants of linear chains of carbon and boron nitride. Carbon *150*, 349–355.

31. Mikhailovskij, I.M., Sadanov, E.V., Kotrechko, S., Ksenofontov, V.A., and Mazilova, T.I. (2013). Measurement of the inherent strength of carbon atomic chains. Phys. Rev. B *87*, 045410.

32. Shin, M.K., Lee, B., Kim, S.H., Lee, J.A., Spinks, G.M., Gambhir, S., Wallace, G.G., Kozlov, M.E., Baughman, R.H., and Kim, S.J. (2012). Synergistic toughening of composite fibres by self-alignment of reduced graphene oxide and carbon nanotubes. Nat. Commun. *3*, 650.

33. Henkelman, G., Arnaldsson, A., and Jonsson, H. (2006). A fast and robust algorithm for Bader decomposition of charge density. Comput. Mater. Sci. *36*, 354–360.

34. Manz, T.A. (2017). Introducing DDEC6 atomic population analysis: part 3. Comprehensive method to compute bond orders. RSC Adv. *7*, 45552–45581.

35. Liu, X., Li, Q., Ruan, Q., Rahn, M.S., Yakobson, B.I., and Hersam, M.C. (2022). Borophene synthesis beyond the single-atomic-layer limit. Nat. Mater. *21*, 35–40.

36. Mahabal, M.S., Deshpande, M.D., Hussain, T., and Ahuja, R. (2015). Sensing characteristics of a graphene-like boron carbide monolayer towards selected toxic gases. Chemphyschem *16*, 3511–3517.

37. Qin, J.K., Liao, P.Y., Si, M.W., Gao, S.Y., Qiu, G., Jian, J., Wang, Q.X., Zhang, S.Q., Huang, S.Y., Charnas, A., et al. (2020). Raman response and transport properties of tellurium atomic chains encapsulated in nanotubes. Nat. Electron. *3*, 141–147.

38. Kobayashi, K., and Yasuda, H. (2015). Structural transition of tellurium encapsulated in confined one-dimensional nanospaces depending on the diameter. Chin. Chem. Lett. *634*, 60–65.

39. Huang, H.Y., Zhang, J.Y., Zhang, Y.F., Fu, C.C., Huang, J.L., Cheng, Y.H., Niu, C.M., Zhao, X.L., and Shinohara, H. (2019). Rock-salt and helix structures of silver iodides under ambient conditions. Natl. Sci. Rev. *6*, 767–774.

40. Senga, R., Komsa, H.P., Liu, Z., Hirose-Takai, K., Krasheninnikov, A.V., and Suenaga, K. (2014). Atomic structure and dynamic behaviour of truly one-dimensional ionic chains inside carbon nanotubes. Nat. Mater. *13*, 1050–1054.

41. Zhou, Y., Li, Y., Li, J., Dong, J., and Li, H. (2017). Electronic transport properties of carbon and boron nitride chain heterojunctions. J. Mater. Chem. C *5*, 1165–1178.

42. Yang, F., Li, C., Li, J., Liu, P., and Yang, G. (2021). Carbyne nanocrystal: one-dimensional van der Waals crystal. ACS Nano *15*, 16769–16776.

43. Pan, B., Xiao, J., Li, J., Liu, P., Wang, C., and Yang, G. (2015). Carbyne with finite length: the one-dimensional *sp* carbon. Sci. Adv. *1*, e1500857.

44. Casari, C.S., and Milani, A. (2018). Carbyne: from the elusive allotrope to stable carbon atom wires. MRS Commun. *8*, 207–219.

45. Scheidt, J.H. (2019). Toward the synthesis of highly processable long-chain carbyne using multilevel pulse injection. J. Nanomater. *2019*, 1–8.

46. Kresse, G., and Furthmüller, J. (1996). Efficiency of ab-initio total energy calculations for metals and semiconductors using a plane-wave basis set. Comput. Mater. Sci. *6*, 15–50.

47. Perdew, J.P., Burke, K., and Ernzerhof, M. (1996). Generalized gradient approximation made simple. Phys. Rev. Lett. *77*, 3865–3868.

48. Blöchl, P.E. (1994). Projector augmented-wave method. Phys. Rev. B *50*, 17953.

49. Monkhorst, H.J., and Pack, J.D. (1976). Special points for Brillouin-zone integrations. Phys. Rev. B *13*, 5188.

Matter, Volume *5*

Supplemental information

The strongest and toughest predicted materials:

Linear atomic chains without a Peierls instability

Enlai Gao, Yongzhe Guo, Zhengzhi Wang, Steven O. Nielsen, and Ray H. Baughman

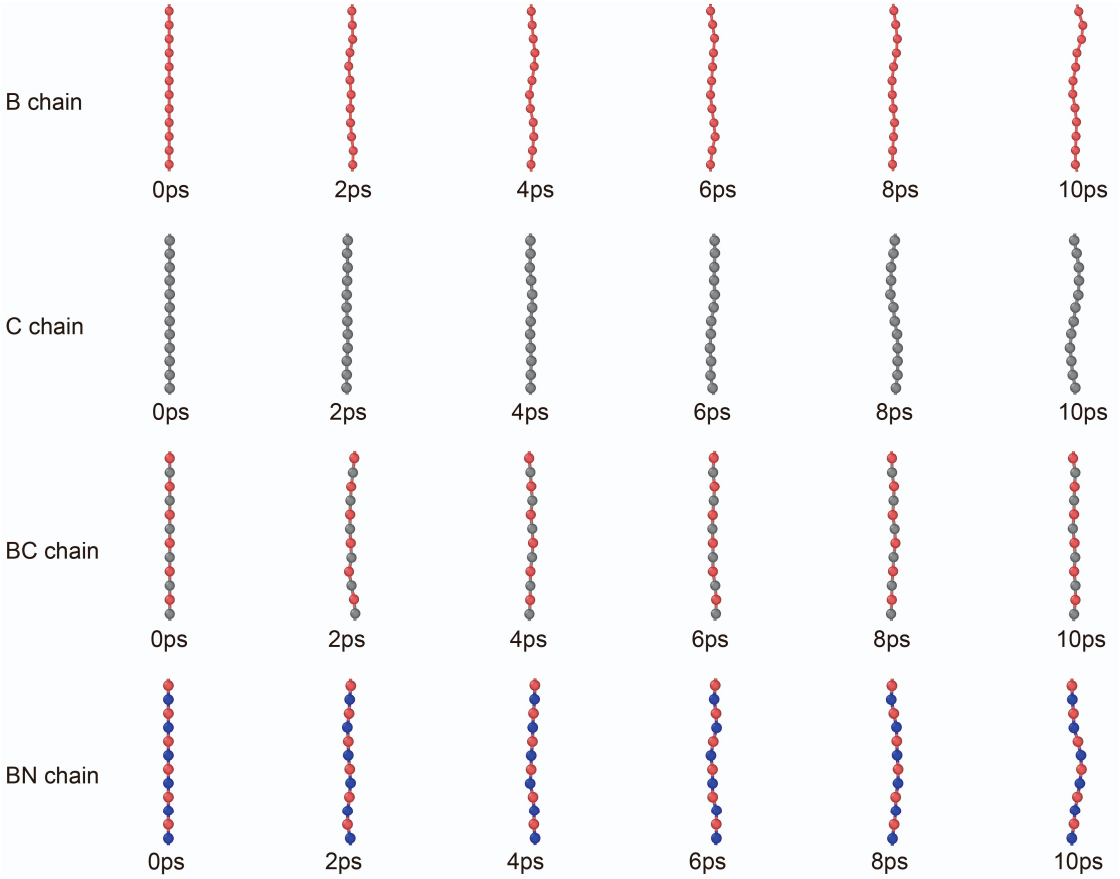

Figure S1. Ab initio molecular dynamics simulations of B, C, BC and BN chains at 300 K for 10 ps.

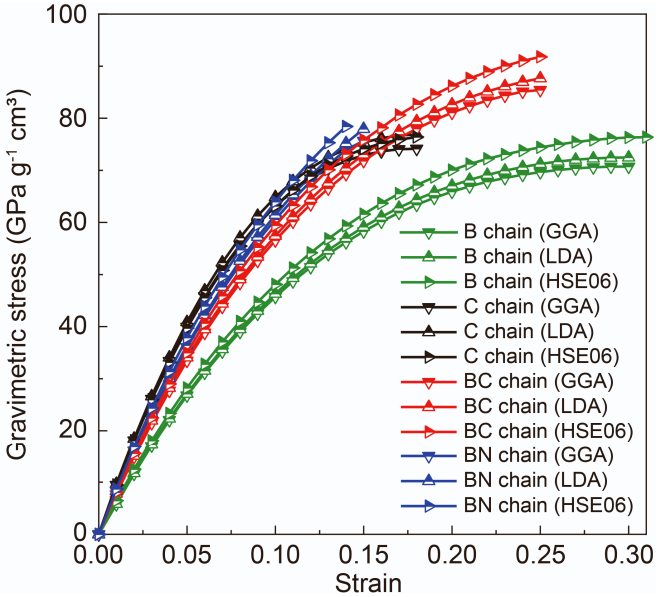

Figure S2. Gravimetric stress vs. strain curves of B, C, BC, and BN chains as a function of strain obtained from DFT calculations with GGA, LDA, and HSE06 functionals.

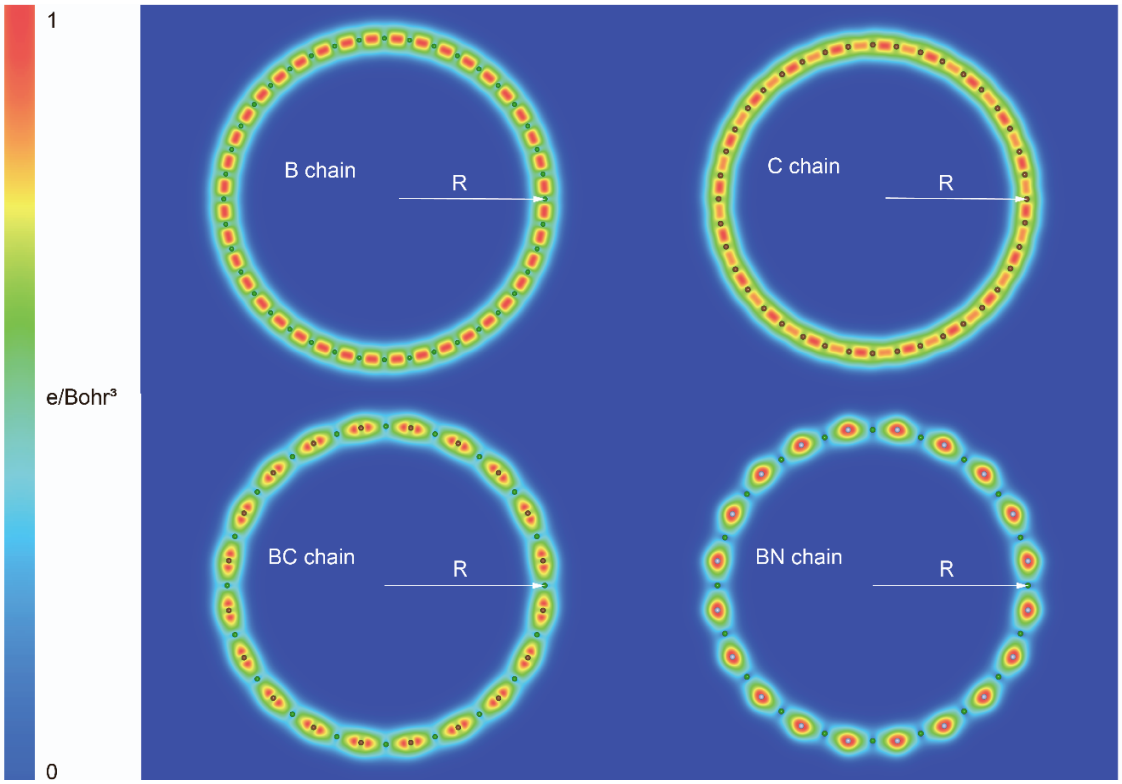

Figure S3. Bending configurations of B, C, BC, and BN chains obtained from DFT calculations.

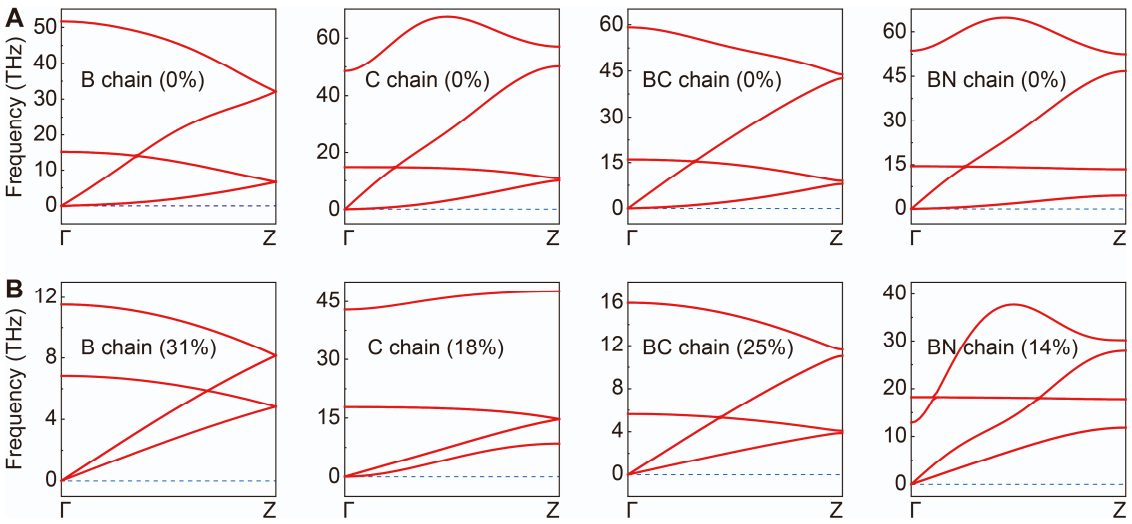

Figure S4. Phonon dispersion curves of linear B, C, BC and BN chains under (A) zero strain and (B) near strain-to-failure.

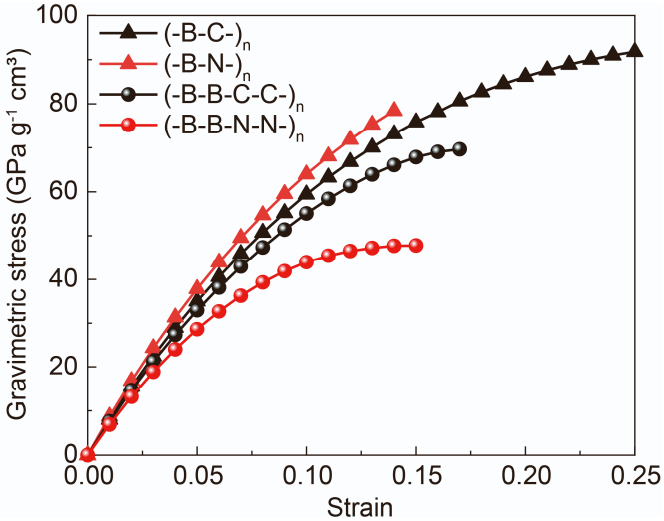

Figure S5. Gravimetric stress-strain curves of $(\text{-B-C-})_n$, $(\text{-B-N-})_n$, $(\text{-B-B-C-C-})_n$, and $(\text{-B-B-N-N-})_n$ chains obtained from DFT calculations, respectively.

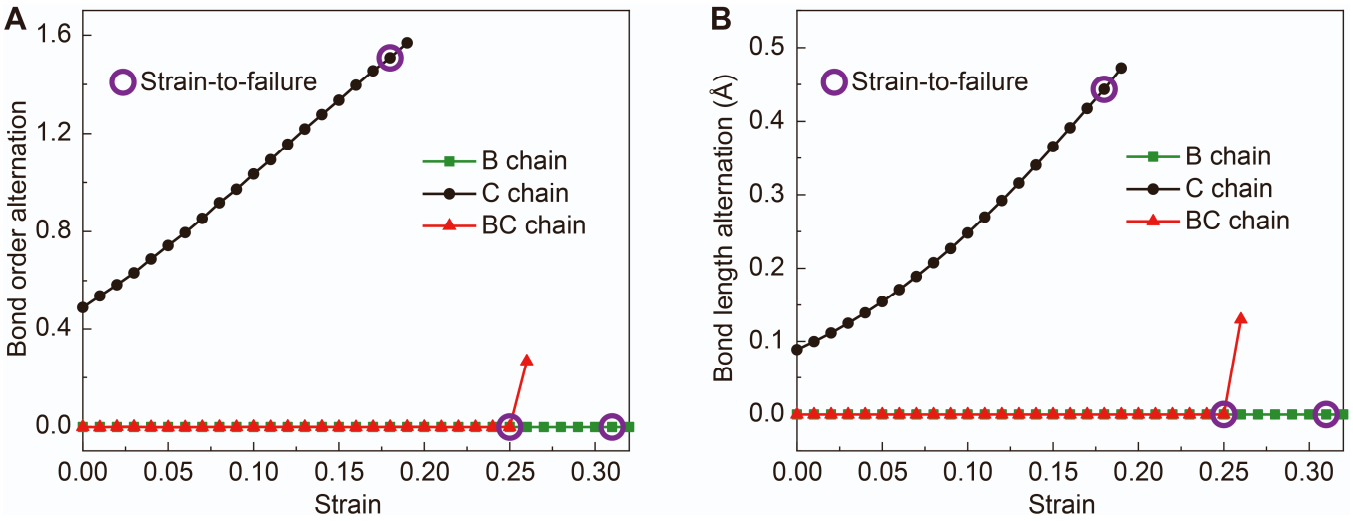

Figure S6. Bond alternation of neighboring bonds in B, C and BC chains as a function of tensile strain. The points at the strain-to-failure are marked with purple circles.

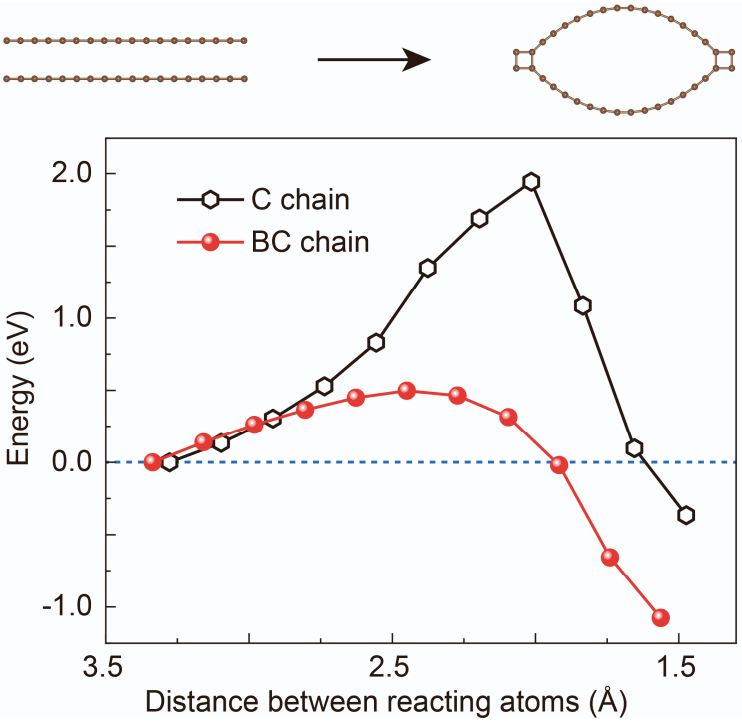

Figure S7. Inter-chain reaction by formation of four-membered rings (top) and the energy change of this reaction per ring as a function of the separation between reacting atoms (bottom).

Table S1. Gravimetric strength (σ_g), gravimetric modulus (Y_g), strain to failure (ε_s), and gravimetric toughness (T) for linear atomic chains compared with other high mechanical performance materials.

Crystals	σ_g (GPa·g^{-1}·cm^3)	Y_g (GPa·g^{-1}·cm^3)	ε_s	T (kJ/g)	Refs
B chain	76.4	643	0.31	16.92	
C chain	76.4	945	0.18	9.43	
BC chain	91.8	802	0.25	15.27	
BN chain	78.4	868	0.14	6.45	
CNT (5, 5)	45.3	441	0.30	10.2	
BNNT (5, 5)	41.0	349	0.28	8.2	
h-BN (zigzag)	44.9	343	0.28	7.67	1-3
Graphene	50.6	453	0.25	8.77	4
MoS_2 (armchair)	4.7	40	0.26	0.82	5,6
Diamond	24.2	327	0.13	2.03	4
Lonsdaleite	37.1	377	0.31	8.61	7,8
w-BN	26.2	249	0.23	4.13	9-11
c-BN	24.2	230	0.22	3.64	9,12,13
BC_3	34.0	165	0.23	4.43	14

REFERENCES

1. Wu, J.T., Wang, B.L., Wei, Y.J., Yang, R.G., and Dresselhaus, M. (2013). Mechanics and mechanically tunable band gap in single-layer hexagonal boron-nitride. Mater. Res. Lett. *1*, 200-206.
2. Wang, R., Pan, W., Jiang, M., Chen, J., and Luo, Y. (2002). Investigation of the physical and mechanical properties of hot-pressed machinable Si_3N_4/*h*-BN composites and FGM. Mater. Sci. Eng. B *90*, 261-268.
3. Hao, T., Zhang, Z., Ahmed, T., Xu, J., Brown, S., and Hossain, Z.M. (2021). Line-defect orientation- and length-dependent strength and toughness in *h*BN. J. Appl. Phys. *129*, 014304.
4. Shao, Q., Li, R.S., Yue, Z.G., Wang, Y.L., and Gao, E.L. (2021). Data-driven discovery and understanding of ultrahigh-modulus crystals. Chem. Mater. *33*, 1276-1284.
5. Worsley, M.A., Shin, S.J., Merrill, M.D., Lenhardt, J., Nelson, A.J., Woo, L.Y., Gash, A.E., Baumann, T.F., and Orme, C.A. (2015). Ultralow density, monolithic WS_2, MoS_2, and MoS_2/graphene aerogels. ACS Nano *9*, 4698-4705.
6. Gan, Y.Y., and Zhao, H.J. (2014). Chirality effect of mechanical and electronic properties of monolayer MoS_2 with vacancies. Phys. Lett. A *378*, 2910-2914.
7. Kulnitskiy, B., Perezhogin, I., Dubitsky, G., and Blank, V. (2013). Polytypes and twins in the diamond-lonsdaleite system formed by high-pressure and high-temperature treatment of graphite. Acta. Crystallogr. B Mater. *69*, 474-479.
8. Li, Q., Sun, Y., Li, Z., and Zhou, Y. (2011). Lonsdaleite – A material stronger and stiffer than diamond. Scr. Mater. *65*, 229-232.
9. Zhang, R.F., Veprek, S., and Argon, A.S. (2008). Anisotropic ideal strengths and chemical bonding of wurtzite BN in comparison to zincblende BN. Phys. Rev. B *77*, 172103.
10. Deura, M., Kutsukake, K., Ohno, Y., Yonenaga, I., and Taniguchi, T. (2017). Nanoindentation measurements of a highly oriented wurtzite-type boron nitride bulk crystal. Jpn. J. Appl. Phys. *56*, 030301.
11. Sōma, T., Sawaoka, A., and Saito, S. (1974). Characterization of wurtzite type boron nitride synthesized by shock compression. Mater. Res. Bull. *9*, 755-762.
12. Bohr, S., Haubner, R., and Lux, B. (1995). Comparative aspects of c-BN and diamond CVD. Diamond Relat. Mater. *4*, 714-719.
13. Richter, F., Herrmann, M., Molnar, F., Chudoba, T., Schwarzer, N., Keunecke, M., Bewilogua, K., Zhang, X.W., Boyen, H.G., and Ziemann, P. (2006). Substrate influence in Young's modulus determination of thin films by indentation methods: Cubic boron nitride as an example. Surf. Coat. Technol. *201*, 3577-3587.
14. Zhang, M., Liu, H., Li, Q., Gao, B., Wang, Y., Li, H., Chen, C., and Ma, Y. (2015). Superhard BC_3 in cubic diamond structure. Phys. Rev. Lett. *114*, 015502.